

# Global convergence analysis of Caputo fractional Whittaker method with real world applications

SAPAN KUMAR NAYAK<sup>1</sup> 

P. K. PARIDA<sup>1,✉</sup> 

<sup>1</sup>*Department of Mathematics,  
Central University of Jharkhand,  
Ranchi-835222, India.*

*sapannayak7@gmail.com*

*pkparida@cuj.ac.in*

## ABSTRACT

The present article deals with the effect of convexity in the study of the well-known Whittaker iterative method, because an iterative method converges to a unique solution  $t^*$  of the nonlinear equation  $\psi(t) = 0$  faster when the function's convexity is smaller. Indeed, fractional iterative methods are a simple way to learn more about the dynamic properties of iterative methods, *i.e.*, for an initial guess, the sequence generated by the iterative method converges to a fixed point or diverges. Often, for a complex root search of nonlinear equations, the selective real initial guess fails to converge, which can be overcome by the fractional iterative methods. So, we have studied a Caputo fractional double convex acceleration Whittaker's method (CFDCAWM) of order at least  $(1 + 2\zeta)$  and its global convergence in broad ways. Also, the faster convergent CFDCAWM method provides better results than the existing Caputo fractional Newton method (CFNM), which has  $(1 + \zeta)$  order of convergence. Moreover, we have applied both fractional methods to solve the nonlinear equations that arise from different real-life problems.

**RESUMEN**

El presente artículo trata con el efecto de la convexidad en el estudio del bien conocido método iterativo de Whittaker, puesto que un método iterativo converge a una única solución  $t^*$  de una ecuación no-lineal  $\psi(t) = 0$  más rápidamente cuando la convexidad de la función es más pequeña. De hecho, métodos iterativos fraccionarios son una manera simple de aprender más sobre las propiedades dinámicas de los métodos iterativos, *i.e.*, para una suposición inicial, la sucesión generada por el método iterativo converge a un punto fijo o diverge. A menudo, para búsquedas de raíces complejas de ecuaciones no-lineales, la suposición inicial real elegida no converge, lo que se puede superar usando métodos iterativos fraccionarios. Así, hemos estudiado un método de Whittaker con aceleración convexa doble Caputo fraccionario (CFD-CAWM) de orden al menos  $(1 + 2\zeta)$  y su convergencia global de manera amplia. También el método convergente CFD-CAWM más rápido entrega mejores resultados que el método de Newton Caputo fraccionario (CFNM) existente, que tiene orden de convergencia  $(1 + \zeta)$ . Más aún, hemos aplicado ambos métodos fraccionarios para resolver ecuaciones no-lineales que aparecen en diferentes problemas de la vida real.

**Keywords and Phrases:** Fractional derivative, efficiency index, nonlinear equations, Newton's method, Whittaker's method, convergence plane, basin of attraction.

**2020 AMS Mathematics Subject Classification:** 65H105, 26A33.

## 1 Introduction

In 1695, two famous mathematicians changed the concept of calculus when they came up with the fractional derivative. Fortunately, L'Hospital had raised a question in a letter to Leibniz, and in the letter, both of them discussed their ideas about the possibilities of semi-derivative function. Since then, there have been vast changes in the theory of fractional calculus and its real-world applications. Thus, fractional calculus builds useful tools in many real-world applications such as science, engineering, economics, medicine, and other fields (see, [1, 3, 10, 18, 19, 22, 29]).

Generally, we know that the classical work in mathematics is to solve the nonlinear equation

$$\psi(t) = 0, \quad (1.1)$$

where  $\psi$  is a real-valued function of a real variable. This task becomes more difficult when the degree of polynomials is greater than or equal to five, or it is a transcendental equation. In general, as there are no analytical methods to handle the above equation, the demand for iterative methods has increased day by day in the last few decades. The most suitable method to solve nonlinear equations, as we know, is quadratic convergent Newton's method (NM):

$$\begin{cases} t_0 & \text{given,} \\ t_{n+1} = t_n - \frac{\psi(t_n)}{\psi'(t_n)}, & n \geq 0. \end{cases} \quad (1.2)$$

Indeed, using iterative methods to solve (1.1) is more suitable and reliable, and it is also true that by using these methods, we can obtain many significant numerical results and related information about nonlinear equations. The effect of fractional derivative on NM was first deduced by Brambila *et al.* [30], who observed that the fractional Newton method (FNM) keeps the ability to search the complex roots of a polynomial even if we choose a real suitable initial guess. By deepening the fractional order, the complex roots of the polynomial are hidden. The nature of fractional iterative methods is that they can locate the positions of different polynomial roots in a different order of derivative. In the year 2019, Akgül *et al.* [2], studied the FNM

$$t_{n+1} = t_n - \left( \Gamma(\zeta + 1) \frac{\psi(t_n)}{\mathcal{C}\mathcal{D}_a^\zeta \psi(t_n)} \right),$$

and proved its order of convergence as  $2\zeta$ . Later, Candelario *et al.* [7] modified the FNM to a better form

$$t_{n+1} = t_n - \left( \Gamma(\zeta + 1) \frac{\psi(t_n)}{\mathcal{C}\mathcal{D}_a^\zeta \psi(t_n)} \right)^{\frac{1}{\zeta}}$$

with order of convergence  $(1+\zeta)$ . They tested the FNM on some numerical examples and provided good results with its dynamics, too.

If we see some research papers (for example, [11, 14, 32]), we can see how the influence of convexity on a real function enhanced the order of convergence. Moreover, the smaller convexity of a nonlinear equation causes the faster convergence of (1.2) to a unique solution  $t^*$  of a nonlinear equation. The classical double convex acceleration of the Whittaker method [32] employing convexity is given below:

$$t_{n+1} = t_n - \frac{1}{4} \left( 2 - L_\psi(t_n) + \frac{4 + 2L_\psi(t_n)}{2 - L_\psi(t_n)(2 - L_\psi(t_n))} \right) \frac{\psi(t_n)}{\psi'(t_n)} \quad (1.3)$$

where  $L_\psi(t_n) = \frac{\psi(t)\psi''(t)}{(\psi'(t))^2}$ . The cubic order convergence method developed by Whittaker is a simplified version of the method developed by Newton. It is also known as the parallel-chord method, which comes from its geometric interpretation of functions. It is known [12], that if we have an iterative process  $t_{n+1} = F(t_n)$  with  $t_{n+1} = t_n - \frac{\psi(t_n)}{\psi'(t_n)} H(L_\psi(t_n))$  and  $H(0) = 1$ ,  $H'(0) = \frac{1}{2}$  and  $|H''(0)| < +\infty$ , it has a third order convergence.

In this paper, we have introduced a new convex acceleration of the Whittaker method using the concept of the Caputo fractional derivative, that is, the Caputo fractional double convex acceleration of the Whittaker method (CFDCAWM). Hence, our main aim in the present article is to investigate further the global convergence analysis, stability, and reliability of CFDCAWM. A detailed comparison of the Caputo fractional Newton method (CFNM) and the CFDCAWM with some good numerical examples is provided, with the order of convergence of CFDCAWM being at least  $(1 + 2\zeta)$ .

The remaining part of the article is assembled in the following manner: Section 2 includes some primary results and information regarding our method. In Section 3, we provide the order of convergence of the proposed method, and its subsection contains details of the efficiency of our method. Section 4 is devoted to the numerical results of the proposed method with real-life applications and their corresponding convergence planes. Finally, the conclusion of the paper ends with Section 5.

## 2 Basic definitions and results

For centuries, the concept of a non-integer order type derivative has been crucial in many research areas. Also, there are so many definitions and formulas in fractional calculus. For our present work, we have just discussed some of them.

**Definition 2.1** (Gamma function [20]). *The gamma function is a generalized idea of the factorial function, and is defined as follows:*

$$\Gamma(t) = \begin{cases} (t-1)!, & t \in \mathbb{N} \\ \int_0^{+\infty} s^{t-1} e^{-s} ds, & \text{whenever } t > 0. \end{cases}$$

**Definition 2.2** (Riemann-Liouville fractional derivative [16]). *Suppose the function  $\psi : \mathbb{R} \rightarrow \mathbb{R}$  and  $\psi \in \mathcal{L}^1([a, t])$  ( $-\infty < a < t < +\infty$ ) be integrable with  $\zeta \geq 0$  and  $k = [\zeta] + 1$ . Then the Riemann-Liouville fractional derivative (RLFD) of  $\psi(t)$  at  $\zeta$ th order is defined as below:*

$$(\mathcal{D}_{a+}^{\zeta})\psi(t) = \begin{cases} \frac{1}{\Gamma(k-\zeta)} \frac{d^k}{dt^k} \int_a^t \frac{\psi(x)}{(t-x)^{\zeta-k+1}} dx, & \zeta \notin \mathbb{N} \\ \frac{d^{k-1}\psi(t)}{dt^{k-1}}, & \zeta = k-1 \in \mathbb{N} \cup \{0\}. \end{cases}$$

And the reverse process of RLFD is Caputo fractional derivative, which is shown below.

**Definition 2.3** (Caputo fractional derivative [8]). *Consider the function  $\psi : \mathbb{R} \rightarrow \mathbb{R}$ ,  $\psi \in C^{+\infty}([a, t])$  ( $-\infty < a < t < +\infty$ ) with  $\zeta \geq 0$  and  $k = [\zeta] + 1$ , where  $[\zeta]$  is the integer part of  $\zeta$ , then the Caputo fractional derivative (CFD) of  $\psi(t)$  at  $\zeta$ th order can be given as:*

$$(\mathcal{C}^{\mathcal{D}_a^{\zeta}})\psi(t) = \begin{cases} \frac{1}{\Gamma(k-\zeta)} \int_a^t \frac{d^k \psi(x)}{dx^k} \frac{dx}{(t-x)^{\zeta-k+1}}, & \zeta \notin \mathbb{N} \\ \frac{d^{k-1}\psi(t)}{dt^{k-1}}, & \zeta = k-1 \in \mathbb{N} \cup \{0\}. \end{cases}$$

The main difference between RLFD and CFD is, the fractional derivative of a constant function is non-zero in RLFD. On the other hand, Caputo fractional derivative of a constant function is zero. Hence, the nature of the Caputo derivative is, it coincides with the classical derivative. So, our experiments use the CFD with the value  $\zeta \in (0, 1]$ .

**Theorem 2.4** ([24, Proposition 26]). *Let  $\psi(t) = (t-a)^\lambda$ ,  $\zeta \geq 0$ ,  $k = [\zeta] + 1$ , and  $\lambda \in \mathbb{R}$ . Then the RLFD of  $\psi(t)$  of  $\zeta$ th order is:*

$$\mathcal{D}_{a+}^{\zeta}(t-a)^\lambda = \frac{\Gamma(\lambda+1)}{\Gamma(\lambda+1-\zeta)}(t-a)^{\lambda-\zeta}.$$

The next theorem discusses the relation between RLFD and CFD of a function.

**Theorem 2.5** ([24, Proposition 31]). *Suppose  $\psi(t)$  be a function whose CFD and RLFD exist of order  $\zeta \notin \mathbb{N}$  such that  $\zeta \geq 0$ ,  $k = 1 + [\zeta]$ . Then the following equality hold*

$$\mathcal{C}^{\mathcal{D}_a^{\zeta}}\psi(t) = \mathcal{D}_{a+}^{\zeta}\psi(t) - \sum_{j=0}^{k+1} \frac{\psi^{(j)}(a)}{\Gamma(j+1-\zeta)}(t-a)^{j-\zeta}, \quad t > a.$$

With preceding results, we can say  $\mathcal{C}^{\mathcal{D}_a^{\zeta}}(t-a)^k = \mathcal{D}_a^{\zeta}(t-a)^k$ ,  $k = 1, 2, \dots$

*Proof.* A function  $\psi(t)$  with a residual term near point ‘a’ has the following Taylor series:

$$\psi(t) = \sum_{j=0}^{\alpha-1} \frac{t^j}{\Gamma(j+1)} \psi^{(j)}(a) + R_{\alpha-1},$$

where

$$R_{\alpha-1} = \frac{1}{\Gamma(\alpha)} \int_0^t \psi^{(\alpha)}(\theta)(t-\theta)^{\alpha-1} d\theta = I^\alpha \psi^{(\alpha)}(t).$$

Then, applying the linearity property of RLFD, we have

$$\begin{aligned} \mathcal{D}_{a+}^\zeta \psi(t) &= \mathcal{D}_{a+}^\zeta \left( \sum_{j=0}^{\alpha-1} \frac{\psi^{(j)}}{\Gamma(j+1)} \psi^{(j)}(a) + R_{\alpha-1} \right) = \sum_{j=0}^{\alpha-1} \frac{\mathcal{D}_{a+}^{\zeta} t^j}{\Gamma(j+1)} \psi^{(j)}(a) + \mathcal{D}_{a+}^\zeta R_{\alpha-1} \\ &= \sum_{j=0}^{\alpha-1} \frac{\Gamma(j+1)t^{j-\zeta}}{\Gamma(j-\zeta+1)\Gamma(j+1)} \psi^{(j)}(a) + \mathcal{D}_{a+}^\zeta I^\alpha \psi^{(\alpha)}(t) \\ &= \sum_{j=0}^{\alpha-1} \frac{t^{j-\zeta}}{\Gamma(j-\zeta+1)} \psi^{(j)}(a) + I^{j-\zeta} \psi^{(\alpha)}(t) = \sum_{j=0}^{\alpha-1} \frac{t^{j-\zeta}}{\Gamma(j-\zeta+1)} \psi^{(j)}(a) + \mathcal{C}^{\mathcal{D}_a^\zeta} \psi(t). \quad \square \end{aligned}$$

The following theorem represents the fractional-order Taylor series, the extended version of the classical Taylor's theorem.

**Theorem 2.6** ([23]). *Let us assume that  $m$ th order Caputo derivative  $\mathcal{C}^{\mathcal{D}_a^{m\zeta} p(t)} \in C([a, b])$ , for  $m = 1, 2, \dots, k+1$ , where  $0 < \zeta \leq 1$ . Then, the generalized Taylor's formula is given as below:*

$$p(t) = \sum_{j=0}^k \mathcal{C}^{\mathcal{D}_a^{j\zeta} p(a)} \frac{(t-a)^{j\zeta}}{\Gamma(j\zeta+1)} + \mathcal{C}^{\mathcal{D}^{(k+1)\zeta} p(\eta)} \frac{(t-a)^{(k+1)\zeta}}{\Gamma((k+1)\zeta+1)},$$

for  $a \leq \eta \leq t, \forall t \in (a, b]$ , where  $\mathcal{C}^{\mathcal{D}_a^{k\zeta}} = \mathcal{C}^{\mathcal{D}_a^\zeta} \dots \mathcal{C}^{\mathcal{D}_a^\zeta}$  ( $k$ -times). Thus, we can conclude that the Taylor series of  $\psi(t)$  around  $t^*$ , by using Caputo fractional derivative is given as follows:

$$\psi(t) = \frac{\mathcal{C}^{\mathcal{D}_{t^*}^\zeta \psi(t^*)}}{\Gamma(\zeta+1)} [(t-t^*)^\zeta + B_2(t-t^*)^{2\zeta} + B_3(t-t^*)^{3\zeta}] + \mathcal{O}((t-t^*)^{3\zeta}),$$

where

$$B_j = \frac{\Gamma(\zeta+1)}{\Gamma(j\zeta+1)} \frac{\mathcal{C}^{\mathcal{D}_{t^*}^{j\zeta} \psi(t^*)}}{\mathcal{C}^{\mathcal{D}_{t^*}^\zeta \psi(t^*)}}, \quad \text{for } j \geq 2.$$

### 3 Convergence analysis of CFDCAWM

In this paper section, we have generalized the double convex acceleration of Whittaker's method (DCAWM) to CFDCAWM using the Caputo fractional derivative. The following theorem shows the convergence of the proposed method CFDCAWM with its order of convergence. Based on the definition of the Caputo derivative, CFDCAWM can be derived as in the following theorem:

**Theorem 3.1.** *Suppose  $\psi: \mathcal{D} \subseteq \mathbb{R} \rightarrow \mathbb{R}$  be a continuous function, and for any  $\zeta \in (0, 1]$  in the domain  $\mathcal{D}$ , it has  $m$ -order fractional derivatives,  $m \in \mathbb{N}$ . If  $t^*$  is a solution of the equation  $\psi(t) = 0$*

and  $\mathcal{C}^{\mathcal{D}_{t^*}^{\zeta} \psi(t)}$  is non-zero continuous function at  $t^*$ , then the method

$$t_{n+1} = t_n - \left( \Gamma(\zeta + 1) \left( 2 - 2\mathcal{T}\mathcal{C}^{L_{\psi}^{\zeta} t_n} + \frac{4 + 4\mathcal{T}\mathcal{C}^{L_{\psi}^{\zeta} t_n}}{2 - \mathcal{C}^{L_{\psi}^{\zeta} t_n} (4\mathcal{T} - 2\mathcal{T}\mathcal{C}^{L_{\psi}^{\zeta} t_n})} \right) \frac{\psi(t_n)}{4\mathcal{C}^{\mathcal{D}_{t_n}^{\zeta} \psi(t_n)}} \right)^{\frac{1}{\zeta}}$$

having at least  $(1 + 2\zeta)$  order of convergence only if  $\mathcal{T} = \frac{\Gamma(2\zeta+1) - \Gamma^2(\zeta+1)}{\Gamma(2\zeta+1)}$ . The desired error equation is mentioned as below:

$$\begin{aligned} e_{n+1} &= \frac{1}{\zeta} \left[ -\Gamma(2\zeta + 1) \left( 1 - \frac{\Gamma(2\zeta + 1)}{\Gamma^4(\zeta + 1)} \right) B_2^2 \right. \\ &\quad + \frac{\mathcal{T}\Gamma(2\zeta + 1)}{\Gamma^3(\zeta + 1)} \left( 2 - \frac{3\Gamma(2\zeta + 1)}{\Gamma^2(\zeta + 1)} - \frac{(3\mathcal{T} - \frac{1}{2})\Gamma(2\zeta + 1)}{\Gamma^2(\zeta + 1)} \right) B_2^2 \\ &\quad \left. + \frac{1}{\Gamma(\zeta + 1)} \left( 1 + \frac{\mathcal{T}\Gamma(3\zeta + 1)}{\Gamma^3(\zeta + 1)} - \frac{\Gamma(3\zeta + 1)}{\Gamma(\zeta + 1)\Gamma(2\zeta + 1)} \right) B_3 \right] e_n^{1+2\zeta} + \mathcal{O}(e_n^{1+3\zeta}). \end{aligned}$$

*Proof.* With the help of Theorems 2.4 and 2.6, the fractional Taylor's series expansion of the nonlinear function  $\psi(t_n)$  using CFD around  $t^*$  is

$$\psi(t_n) = \frac{\mathcal{C}^{\mathcal{D}_{t^*}^{\zeta} \psi(t^*)}}{\Gamma(\zeta + 1)} [e_n^{\zeta} + B_2 e_n^{2\zeta} + B_3 e_n^{3\zeta}] + \mathcal{O}(e_n^{4\zeta}). \tag{3.1}$$

Also, the first and second Caputo derivatives can be given as:

$$\mathcal{C}^{\mathcal{D}_{t_n}^{\zeta} \psi(t_n)} = \frac{\mathcal{C}^{\mathcal{D}_{t^*}^{\zeta} \psi(t^*)}}{\Gamma(\zeta + 1)} \left[ \Gamma(\zeta + 1) + \frac{\Gamma(2\zeta + 1)}{\Gamma(\zeta + 1)} B_2 e_n^{\zeta} + \frac{\Gamma(3\zeta + 1)}{\Gamma(2\zeta + 1)} B_3 e_n^{2\zeta} \right] + \mathcal{O}(e_n^{3\zeta}), \tag{3.2}$$

and

$$\mathcal{C}^{\mathcal{D}_{t_n}^{2\zeta} \psi(t_n)} = \frac{\mathcal{C}^{\mathcal{D}_{t^*}^{\zeta} \psi(t^*)}}{\Gamma(\zeta + 1)} \left[ \Gamma(2\zeta + 1) B_2 + \frac{\Gamma(3\zeta + 1)}{\Gamma(\zeta + 1)} B_3 e_n^{\zeta} \right] + \mathcal{O}(e_n^{2\zeta}). \tag{3.3}$$

Squaring the equation (3.2), we have

$$\begin{aligned} (\mathcal{C}^{\mathcal{D}_{t_n}^{\zeta} \psi(t_n)})^2 &= \left( \frac{\mathcal{C}^{\mathcal{D}_{t^*}^{\zeta} \psi(t^*)}}{\Gamma(\zeta + 1)} \right)^2 \left[ \Gamma^2(\zeta + 1) + 2\Gamma(2\zeta + 1) B_2 e_n^{\zeta} \right. \\ &\quad \left. + \left( \frac{\Gamma^2(2\zeta + 1)}{\Gamma^2(\zeta + 1)} B_2^2 + \frac{2\Gamma(\zeta + 1)\Gamma(3\zeta + 1)}{\Gamma(2\zeta + 1)} B_3 \right) e_n^{2\zeta} + \frac{2\Gamma(2\zeta + 1)\Gamma(3\zeta + 1)}{\Gamma(\zeta + 1)\Gamma(2\zeta + 1)} B_2 B_3 e_n^{3\zeta} \right] + \mathcal{O}(e_n^{4\zeta}). \end{aligned} \tag{3.4}$$

Also from the equations (3.1) and (3.2), we get

$$\begin{aligned} \frac{\psi(t_n)}{\mathcal{C}^{\mathcal{D}_{t_n}^{\zeta} \psi(t_n)}} &= \frac{1}{\Gamma(\zeta + 1)} \left[ e_n^{\zeta} + \frac{\Gamma^2(\zeta + 1) - \Gamma(2\zeta + 1)}{\Gamma^2(\zeta + 1)} B_2 e_n^{2\zeta} \right. \\ &\quad \left. + \left[ \left( \frac{\Gamma^2(2\zeta + 1)}{\Gamma^4(\zeta + 1)} - \frac{\Gamma(2\zeta + 1)}{\Gamma^2(\zeta + 1)} \right) B_2^2 + \left( \frac{\Gamma(\zeta + 1)\Gamma(2\zeta + 1) - \Gamma(3\zeta + 1)}{\Gamma(\zeta + 1)\Gamma(2\zeta + 1)} \right) B_3 \right] e_n^{3\zeta} \right] + \mathcal{O}(e_n^{4\zeta}). \end{aligned}$$

Combining (3.1) and (3.3), we obtain

$$\psi(t_n) \mathcal{C}^{\mathcal{D}_{t_n}^{2\zeta} \psi(t_n)} = \left( \frac{\mathcal{C}^{\mathcal{D}_{t^*}^{\zeta} \psi(t^*)}}{\Gamma(\zeta + 1)} \right)^2 \left[ \Gamma(2\zeta + 1) B_2 e_n^{\zeta} + \left( B_2^2 \Gamma(2\zeta + 1) + \frac{\Gamma(3\zeta + 1)}{\Gamma(\zeta + 1)} B_3 \right) e_n^{2\zeta} \right] + \mathcal{O}(e_n^{3\zeta}).$$

Using (3.4) in the above equation, the Taylor expansion of  $\mathcal{C}^{L_\psi^\zeta \psi(t_n)}$  around  $t^*$  can be given as:

$$\mathcal{C}^{L_\psi^\zeta t_n} = \frac{\Gamma(2\zeta + 1)}{\Gamma^2(\zeta + 1)} B_2 e_n^\zeta + \frac{1}{\Gamma^2(\zeta + 1)} \left[ B_2^2 \Gamma(2\zeta + 1) + \frac{\Gamma(3\zeta + 1)}{\Gamma(\zeta + 1)} B_3 - 2 \frac{1}{\Gamma^2(\zeta + 1)} \Gamma^2(2\zeta + 1) B_2^2 \right] e_n^{2\zeta} + \mathcal{O}(e_n^{3\zeta}).$$

Squaring the above term, we get

$$\left( \mathcal{C}^{L_\psi^\zeta t_n} \right)^2 = \frac{\Gamma^2(2\zeta + 1)}{\Gamma^4(\zeta + 1)} B_2^2 e_n^{2\zeta} + \mathcal{O}(e_n^{3\zeta}).$$

Thus

$$\begin{aligned} \mathcal{C}^{L_\psi^\zeta t_n} \frac{\psi(t_n)}{\mathcal{D}_{t^*}^\zeta \psi(t_n)} &= \frac{1}{\Gamma^3(\zeta + 1)} \left[ \Gamma(2\zeta + 1) B_2 e_n^{2\zeta} + \left\{ 2 \left( \Gamma(2\zeta + 1) - \Gamma^2(2\zeta + 1) - \frac{\Gamma^2(2\zeta + 1)}{2\Gamma^2(\zeta + 1)} \right) B_2^2 \right. \right. \\ &\quad \left. \left. + \frac{\Gamma(3\zeta + 1)}{\Gamma(\zeta + 1)} B_3 \right\} e_n^{3\zeta} \right] + \mathcal{O}(e_n^{4\zeta}). \end{aligned}$$

Now

$$\left( \mathcal{C}^{L_\psi^\zeta t_n} \right)^2 \frac{\psi(t_n)}{\mathcal{D}_{t^*}^\zeta \psi(t_n)} = \frac{\Gamma^2(2\zeta + 1)}{\Gamma^5(\zeta + 1)} B_2^2 e_n^{3\zeta} + \mathcal{O}(e_n^{4\zeta}).$$

By using geometric series expansion, we obtain

$$\begin{aligned} \frac{4 + 4\mathcal{T}\mathcal{C}^{L_\psi^\zeta t_n}}{2 - \mathcal{C}^{L_\psi^\zeta t_n} (4\mathcal{T} - 2\mathcal{T}\mathcal{C}^{L_\psi^\zeta t_n})} &= (2 + 2\mathcal{T}\mathcal{C}^{L_\psi^\zeta t_n}) \left[ 1 - \left( 2 - \mathcal{T}\mathcal{C}^{L_\psi^\zeta t_n} - \mathcal{T} \left( \mathcal{C}^{L_\psi^\zeta t_n} \right)^2 \right) \right]^{-1} \\ &= (2 + 2\mathcal{T}\mathcal{C}^{L_\psi^\zeta t_n}) [1 + E + E^2 + \dots], \end{aligned}$$

$$\text{where, } E = \left[ 2 - \mathcal{T}\mathcal{C}^{L_\psi^\zeta t_n} - \mathcal{T} \left( \mathcal{C}^{L_\psi^\zeta t_n} \right)^2 \right].$$

Finally, we reach to the destination as the error equation is:

$$\begin{aligned} e_{n+1} &= \frac{1}{\zeta} \left[ -\Gamma(2\zeta + 1) \left( 1 - \frac{\Gamma(2\zeta + 1)}{\Gamma^4(\zeta + 1)} \right) B_2^2 \right. \\ &\quad \left. + \frac{\mathcal{T}\Gamma(2\zeta + 1)}{\Gamma^3(\zeta + 1)} \left( 2 - \frac{3\Gamma(2\zeta + 1)}{\Gamma^2(\zeta + 1)} - \frac{(3\mathcal{T} - \frac{1}{2})\Gamma(2\zeta + 1)}{\Gamma^2(\zeta + 1)} \right) B_2^2 \right. \\ &\quad \left. + \frac{1}{\Gamma(\zeta + 1)} \left( 1 + \frac{\mathcal{T}\Gamma(3\zeta + 1)}{\Gamma^3(\zeta + 1)} - \frac{\Gamma(3\zeta + 1)}{\Gamma(\zeta + 1)\Gamma(2\zeta + 1)} \right) B_3 \right] e_n^{1+2\zeta} + \mathcal{O}(e_n^{1+3\zeta}). \end{aligned}$$

This ends the proof. □

### 3.1 Efficiency index

When studying iterative processes, it is important to consider both the speed of convergence (order of convergence) and the computational cost (number of functions and derivative evaluations) required to compute  $t_{n+1}$  from  $t_n$ . The efficiency index of the iterative method explained by Traub [15] is  $\mathcal{E}^* = z^{1/k}$ , where  $z$  plays the role of order of convergence of the method and  $k$  denotes total

functional cost evaluations per each iteration. It can be seen from Figure 1 that both the fractional iterative method's efficiency index increases with increasing the order of derivative  $\zeta$ . Moreover, the maximum value  $\mathcal{E}^*$  found in CFNM and CFDCAWM are 1.414 and 1.442, respectively. So, as illustrated in the figure, the efficiency index curve of CFDCAWM always lies above the CFNM. Hence, the  $(1 + 2\zeta)^{th}$  order method CFDCAWM provides better performance and is more efficient than the  $(1 + \zeta)^{th}$  order method CFNM.

In the next section, we have taken some nonlinear equations for the convergence test of the proposed method and provided more information about the stability and faster convergence of CFDCAWM with some good numerical results and convergence plane.

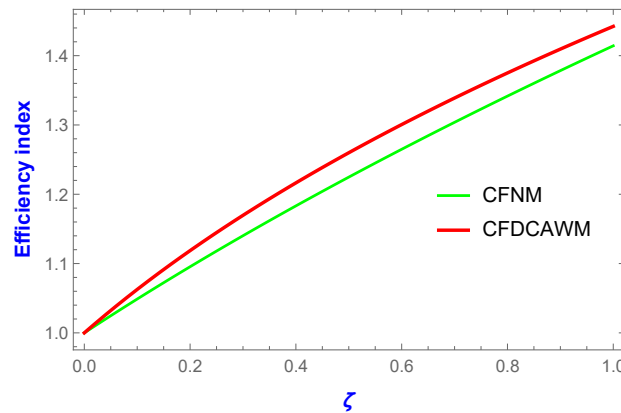


Figure 1: Efficiency indices of CFNM and CFDCAWM.

## 4 CFDCAWM with their numerical results and convergence plane.

To obtain the numerical results of iterative methods, we use Matlab R2018a with the arithmetic of the double-precision procedure to solve different kinds of nonlinear equations. The stopping criteria of the fractional iterative methods are frequently terminated when either  $|t_{n+1} - t_n| < 10^{-6}$  or  $|\psi(t_n)| < 10^{-6}$ , with a maximum of 300 iterations. Using the program made by Paul Godfrey based on [20], we calculate the Gamma function, whose accuracy along the real axis is 15 significant digits and in the complex plane is 13 significant digits. Moreover, the graphical part of this paper, that is, a convergence plane of iterative methods, has been made by using modified algorithms based on [21] in Mathematica 11.1 and a laptop Lenovo Ideapad flex 5, 1.19 GHz Intel(R) Core™ i5-1035G1 CPU. Each convergence plane consists of a mesh of  $400 \times 400$  real and complex points. Different colors (red, blue, green, yellow...) on convergence planes mean different roots, whereas black indicates the divergence of the method.

**Example 4.1** ([13]). A state equation links the gas constant to a gas's pressure, volume, and temperature. In the Beattie-Bridgman equation, experimental constants are employed to allow for the decrease in the effective number of molecules caused by various types of molecular aggregation. In the first test function, we used the Beattie-Bridgman equation, which is as follows:

$$c = \frac{RT}{V} + \frac{\beta}{V^2} + \frac{\gamma}{V^3} + \frac{\delta}{V^4} - P = 0 \quad (4.1)$$

$P$  is atmospheric pressure,  $R$  is gas constant,  $T$  is absolute temperature in  $K$ , and volume  $V$  in  $L/mol$ . For  $T = 273.15K$ ,  $\beta = -1.16584$ ,  $\gamma = 0.0542254$ , and  $\delta = -0.0001251$ . After inserting above values in (4.1), the equation convert to following quartic degree polynomial equation for a pressure of 100 atm:

$$\psi_1(t) = t^4 - 0.22411958 t^3 + 0.011658361 t^2 - 5.422539 \times 10^{-4} t - 1.251 \times 10^{-6}$$

with the roots  $t_1 = -0.0022$ ,  $t_2 = 0.1755$ ,  $t_3 = 0.0254 + 0.0510i$ , and  $t_4 = 0.0254 - 0.0510i$ .

Table 1: Results of CFNM for  $\psi_1(t)$  with initial guess  $t_0 = 1.5$

$\zeta$	$t^*$	$ t_{n+1} - t_n $	$ \psi(t_{n+1}) $	Iterations
0.1	0.178610412640083	2.451188583441066e-06	1.450813559042032e-05	300
0.2	0.177091772811241	1.824477708772809e-06	7.157942621320157e-06	300
0.3	0.176208764373106	1.144633855865163e-06	3.056113886250757e-06	300
0.4	0.175822192040086	9.973031851462366e-07	1.299498966609209e-06	218
0.5	0.175754695139549	3.307545208941498e-06	9.952113269586370e-07	82
0.6	0.175744973843258	1.206591802094259e-05	9.514452435446740e-07	38
0.7	0.175750319786336	3.910969726900193e-05	9.755112797258072e-07	23
0.8	0.175722751968572	9.416356483973876e-05	8.514564575890538e-07	17
0.9	0.175637670869286	1.558852358621021e-04	4.693474071063554e-07	14
1	0.175715573286650	0.003163967768901	8.191721350991289e-07	11

Table 2: Results of CFDCAWM for  $\psi_1(t)$  with initial guess  $t_0 = 1.5$

$\zeta$	$t^*$	$ t_{n+1} - t_n $	$ \psi(t_{n+1}) $	Iterations
0.1	0.178561953323709	2.368122878099177e-06	1.426773613993988e-05	300
0.2	0.177049664573626	1.719411282186112e-06	6.959494002208448e-06	300
0.3	0.176189681978262	1.074871852274617e-06	2.968845997087551e-06	300
0.4	0.175820273163475	9.926277080019030e-07	1.290838413491345e-06	210
0.5	0.175752994062801	3.283711977664083e-06	9.875518627812638e-07	76
0.6	0.175749495618264	1.261041176645050e-05	9.718007971009330e-07	32
0.7	0.175740309046350	3.669505604023127e-05	9.304492295014291e-07	18
0.8	0.175714407451239	8.935095908427226e-05	8.139298489053516e-07	12
0.9	0.175645204608465	1.737789640035292e-04	5.031363206827803e-07	09
1	0.175532814939696	2.402266629901728e-04	6.317771224496375e-12	07

As we can see from Tables 1 and 2, for a real initial guess, the CFDCAWM performs faster with a lower error rate than the CFNM. The minimum number of iterations that reach the root is when  $\zeta$  is close to 1. Furthermore, we have presented the convergence plane with its percentage of convergence for global convergence analysis. The convergence plane is painted with different colors, like  $t_1$  (red),  $t_2$  (green),  $t_3$  (blue), and  $t_4$  (yellow), where the black color represents the divergence. Using the CFNM and CFDCAWM methods, we obtain the percentages of convergence as 86.62% and 86.89%, respectively.

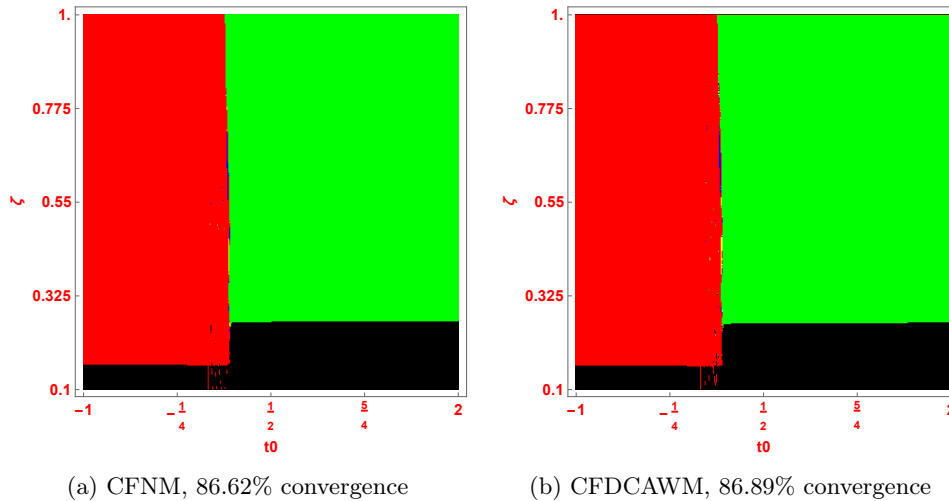


Figure 2: Convergence planes of  $\psi_1(t)$  for real initial guess  $t_0 = a, a \in \mathbb{R}$ .

**Example 4.2** ([9]). *Thermodynamics is an important tool for mechanical engineers and other types of engineers. The zero-pressure specific heat of dry air,  $\mathfrak{C}_p$  kJ/(kg K), is related to temperature (K) by the following polynomial:*

$$\psi_2(t) = 1.9520 \times 10^{-14}t^4 - 9.5838 \times 10^{-11}t^3 + 9.7215 \times 10^{-8}t^2 + 1.671 \times 10^{-4}t + 0.99403$$

having the roots

$$t_1 = -1001.9347479801513 - 1506.1391327465992i,$$

$$t_2 = -1001.9347479801513 + 1506.1391327465992i,$$

$$t_3 = 3456.80155125884 - 1900.6392904677366i,$$

$$t_4 = 3456.80155125884 + 1900.6392904677366i.$$

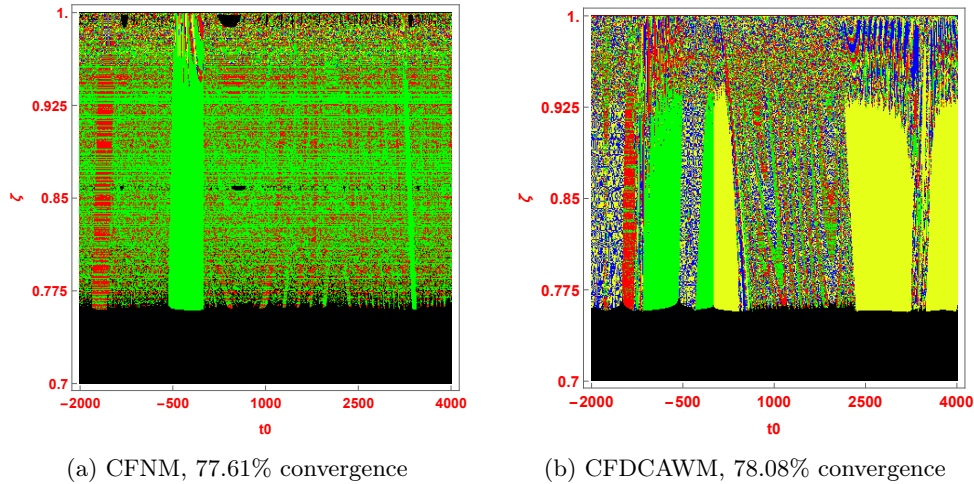
Table 3: Results of CFNMM for  $\psi_2(t)$  with initial guess  $t_0 = 1200$ 

$\zeta$	$t^*$	$ t_{n+1} - t_n $	$ \psi(t_{n+1}) $	Iterations
0.90	-1.0019351270e+03- 1.506139649e+03i	1.68009e-04	9.46029e-07	127
0.91	-1.001934949337910e+03+1.506139772e+03i	2.22485e-04	9.89906e-07	105
0.92	-1.001934982e+03+1.506139634e+03i	2.27315e-04	8.17029e-07	101
0.93	-1.001934996e+03+1.506139613e+03i	2.85064e-04	7.98920e-07	95
0.94	-1.001935115e+03+1.506139440e+03i	3.25671e-04	7.07102e-07	52
0.95	-1.001934691e+03-1.5061397413e+03i	5.72666e-04	9.02668e-07	83
0.96	-1.00193460826e+03+1.506139435e+03i	4.09812e-04	4.92409e-07	48
0.97	-1.001934870e+03+1.506139378e+03i	4.965333e-04	4.05183e-07	46
0.98	-1.001934981e+03+1.506139396e+03i	0.0011022	5.20419e-07	85
0.99	-1.001935145e+03+1.506139393e+03i	0.0035052	7.023826e-07	86
1	-2.278375918070995e+03	1.15764e+03	2.7774308	300

Table 4: Results of CFDCAWM for  $\psi_2(t)$  with initial guess  $t_0 = 1200$ 

$\zeta$	$t^*$	$ t_{n+1} - t_n $	$ \psi(t_{n+1}) $	Iterations
0.90	3.456801942e+03+1.90063953e+03i	1.165819e-04	8.63779e-07	57
0.91	-1.001934857e+03-1.506139637e+03i	1.65497e-04	7.629208e-07	58
0.92	-1.001934909e+03-1.506139589e+03i	1.95917e-04	7.161345e-07	37
0.93	-1.001934830e+03+1.506139574e+03i	2.31665e-04	6.64036e-07	32
0.94	3.456801839e+03+1.900639491e+03i	2.320012e-04	6.55686e-07	28
0.95	3.456801872e+03-1.900639586e+03i	3.96711e-04	8.14106e-07	36
0.96	3.456801709e+03+1.900639507e+03i	3.25045e-04	5.00443e-07	26
0.97	-1.001934720e+03-1.506139406e+03i	4.95736e-04	4.05118e-07	30
0.98	3.456801786e+03+1.9006393777e+03i	7.626349e-04	4.6759e-07	43
0.99	-1.00193501e+03-1.506139695e+03i	0.00469	9.17793e-07	54
1	1.601282223e+05	1.57591e+05	1.24427e+07	300

The CFDCAWM converges quicker than the CFNM, as seen in the Tables 3 and 4. In Figure 3, the convergence plane of the CFDCAWM (78.08%) provide better stability than CFNM (77.61%).

Figure 3: Convergence planes of  $\psi_2(t)$  for real initial guess  $t_0 = a$ ,  $a \in \mathbb{R}$ .

**Example 4.3** ([27]). *Blood is represented as a ‘‘Casson fluid’’, a non-Newtonian fluid. A basic fluid, such as water or blood, will flow through a tube so that the fluid’s central core travels as a plug with little distortion and a velocity gradient towards the tube’s wall, according to the Casson fluid model. The following non-linear polynomial equation has been used to explain the plug flow of Casson fluids, where the change in flow rate is measured by*

$$R = 1 - \frac{16}{7}\sqrt{t} + \frac{4}{3}t - \frac{1}{21}t^4$$

where reduction in flow rate is measure by  $R$ . Take  $R = 0.40$  in the above equation we have the third test function

$$\psi_3(t) = \frac{1}{441}t^8 - \frac{8}{63}t^5 - 0.05714285714t^4 + \frac{16}{9}t^2 - 3.624489796t + 0.36$$

which contains the following roots  $t_1 = 3.82239$ ,  $t_2 = 0.104699$ ,  $t_3 = -2.27869 - 1.98748i$ ,  $t_4 = -2.27869 + 1.98748i$ ,  $t_5 = -1.23877 - 3.40852i$ ,  $t_6 = -1.23877 + 3.40852i$ ,  $t_7 = 1.55392 - 0.940415i$ , and  $t_8 = 1.55392 + 0.94041i$ .

Table 5: Results of CFNM for  $\psi_3(t)$  with initial guess  $t_0 = -0.5 - 0.5i$

$\zeta$	$t^*$	$ t_{n+1} - t_n $	$ \psi(t_{n+1}) $	Iterations
0.1	0.138106293-0.000115792i	1.18425e-04	0.37383	300
0.2	0.138216126-0.000225384i	4.12661e-05	0.10668	300
0.3	0.115361954-0.000027866i	1.80432e-05	0.034481	300
0.4	0.107711638-0.000006849i	7.15017e-06	0.00978	300
0.5	0.105318676-0.000001208i	2.10397e-06	0.00201	300
0.6	0.104830090-0.000000277i	9.962501e-07	4.27483e-04	197
0.7	0.104737418-0.000001542i	9.83237e-07	1.26519e-04	89
0.8	0.104708969-0.000001038i	9.24479e-07	3.37291e-05	41
0.9	0.104700546-0.000000350i	7.36274e-07	6.26827e-06	18
1	0.104698651+0.0i	5.92960e-06	6.23236e-11	05

Table 6: Results of CFDCAWM for  $\psi_3(t)$  with initial guess  $t_0 = -0.5 - 0.5i$

$\zeta$	$t^*$	$ t_{n+1} - t_n $	$ \psi(t_{n+1}) $	Iterations
0.1	0.225782730-0.0009883555i	1.14521e-04	0.36795	300
0.2	0.137305522-0.0000924585i	3.93043e-05	0.10417	300
0.3	0.115118894-0.0000195106i	1.722201e-05	1.72220e-05	300
0.4	0.1076588596-0.0000038959i	6.90493e-06	0.00961	300
0.5	0.1053110124-0.0000004292i	2.05602e-06	0.00199	300
0.6	0.1048302280+0.000000401i	9.98358e-07	4.279307e-04	195
0.7	0.1047374670+0.0000003244i	9.80324e-07	1.26251e-04	88
0.8	0.1047092613+0.0000011816i	9.59435e-07	3.47222e-05	40
0.9	0.1047006008-0.0000001524i	7.48819e-07	6.35958e-06	18
1	0.104698651+0.00000i	0.00103	4.40814e-11	04

The CFDCAWM converges better than the CFNM with complex starting estimate  $t_0 = -0.5 - 0.5i$

and provides less error, as illustrated in Tables 6 and 5.

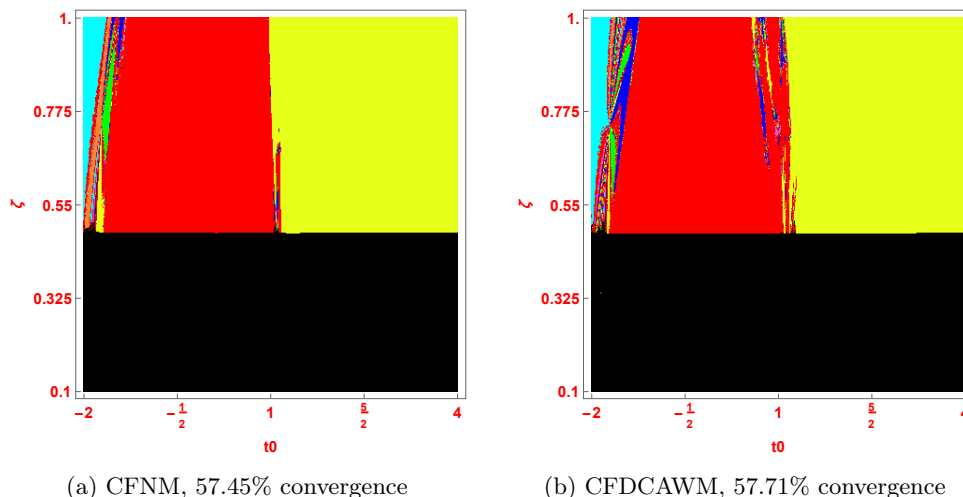


Figure 4: Convergence planes of  $\psi_3(t)$  for complex initial guess  $t_0 = a + ai$ ,  $a \in \mathbb{R}$ .

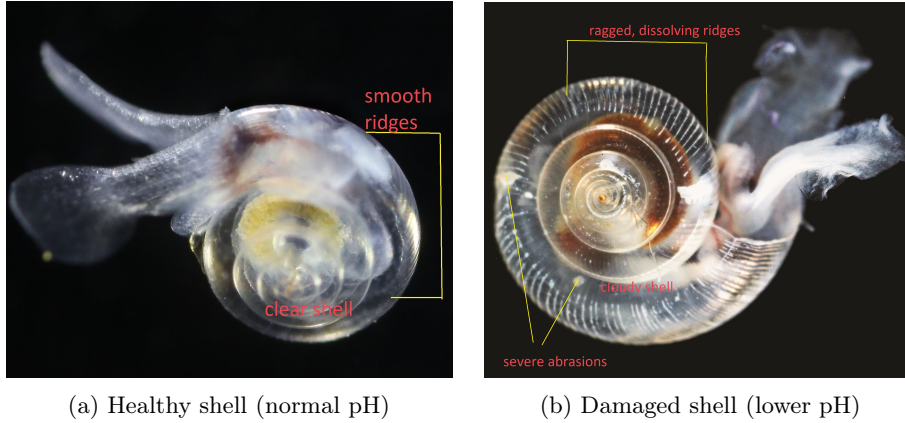
In the Figure 4 convergence planes of  $\psi_3(t)$  are illustrated where the horizontal axis of the graph contains all the complex initial guesses of the form  $t_0 = a + ai$ . The CFDCAWM contains 57.71% and CFNM contains 57.45% region of convergence. To find all most all root in CFNM, the best initial guess  $t_0 \in (-2, -\frac{1}{2})$  but in case of CFDCAWM the best initial guesses lies in  $t_0 \in (-2, -\frac{1}{2})$  and  $t_0 \in (0, 2)$ .

**Example 4.4** ([4]). The increasing pH reduction of Earth's seas due to their absorption of anthropogenic carbon dioxide from the atmosphere is known as "ocean acidification". If alkalinity and temperature remain constant, a 0.1-unit decrease in ocean pH results in a 30% increase in hydrogen ion concentration. The concentration of hydrogen ions increases as a result of a series of chemical reactions that take place when  $CO_2$  is absorbed by saltwater. So, the acidity increases in the seawater and causes carbonate ions to be relatively less abundant. Carbonate ions are vital components of many different kinds of organisms, including the skeletons of coral and seashells.

Lack of carbonate ions can make developing and maintaining shells and other calcium carbonate structures of organisms difficult for calcifying species such as oysters, clams, sea urchins, shallow water corals, deep sea corals, and calcareous plankton.

As  $CO_2$  dissolves in saltwater, the concentration of hydrogen ions  $[H^+]$  rises, which lowers the pH of the ocean as follows:





(a) Healthy shell (normal pH)

(b) Damaged shell (lower pH)

Figure 5: Healthy and damaged pteropod image taken from NOAA website [17].

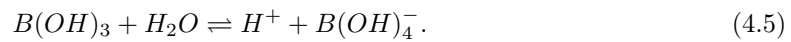
Bicarbonate ions in turn dissociate into carbonate ions  $CO_3^{2-}$ ,



The chemical processes results in hydrogen ions, which add to the acidification. Also,  $H_2O$  separates to form hydrogen ions is given as below



Furthermore, the seawater's boron hydroxide dissociates to release hydrogen ions as



The partial pressure  $\mathcal{P}_t$  of the gas phase  $CO_2$  is measured in ppm by the National Oceanic and Atmospheric Administration (NOAA) at the Mauna Loa Observatory in Hawaii [28], and according to Bacastow and Keeling [5], the equilibrium constants are measured in mol/ltr and the relationship between liquid and gaseous  $CO_2$  is

$$S_0 = \frac{[CO_2]}{\mathcal{P}_t} = 3.347e - 05, \quad (4.6)$$

being the  $[CO_2]$  represent as the sum of the dissolved  $CO_2$ . From the reaction (4.2),

$$S_1 = \frac{[H^+][HCO_3^-]}{[CO_2]} = 9.747e - 07. \quad (4.7)$$

From the reaction (4.3)

$$S_2 = \frac{[H^+][CO_3^{2-}]}{[HCO_3^-]} = 8.501e - 10. \quad (4.8)$$

From the reaction (4.4)

$$S_w = \frac{[H^+]}{[OH^-]} = 6.46e - 15. \quad (4.9)$$

From the reaction (4.5)

$$S_B = \frac{[H^+][B(OH)_4^-]}{[B(OH)_3]} = 1.881e - 09. \quad (4.10)$$

Now the alkanity is

$$\begin{aligned} \mathcal{A} &= \sum(\text{conservative cations}) - \sum(\text{conservative anions}) \\ &= [HCO_3^-] + 2[CO_3^{2-}] + [B(OH)_4^-] + [OH^-] - [H^+]. \end{aligned} \quad (4.11)$$

We can suppose that the values of  $\mathcal{A}$  are independent with time as given in the article [4]. The concentrated  $CO_2$  is evaluated from (4.6) as

$$[CO_2] = S_0 \mathcal{P}_t. \quad (4.12)$$

With the help of equations (4.7) and (4.12), we get

$$[HCO_3^-] = \frac{S_1[CO_2]}{H^+} = \frac{S_0 S_1 \mathcal{P}_t}{[H^+]}. \quad (4.13)$$

In the same way, we can find

$$[CO_3^{2-}] = \frac{S_2[HCO_3^-]}{[H^+]} = \frac{S_0 S_1 S_2 \mathcal{P}_t}{[H^+]^2}. \quad (4.14)$$

Now to find  $[B(OH)_4^-]$  with the help of equations (4.8) and (4.13),

and  $B = [B(OH)_3] + [B(OH)_4^-]$  in (4.10)

$$[B(OH)_4^-] = \frac{BS_B}{S_B + [H^+]}. \quad (4.15)$$

Next, substitute the equations (4.9) and (4.12)-(4.15), we get the alkanity  $\mathcal{A}$  as below:

$$\mathcal{A} = \frac{S_0 S_1 \mathcal{P}_t}{[H^+]} + \frac{2S_0 S_1 S_2 \mathcal{P}_t}{[H^+]^2} + \frac{BS_B}{S_B + [H^+]} + \frac{S_w}{[H^+]} - [H^+].$$

It reduces to the result of the following fourth-degree polynomial equation.

$$p([H^+]) = \sum_{k=0}^4 \Delta_k [H^+]^k, \quad (4.16)$$

where

$$\begin{aligned} \Delta_0 &= 2S_0S_1S_2\mathcal{P}_tS_B, & \Delta_1 &= S_0S_1S_B\mathcal{P}_t + 2S_0S_1S_2\mathcal{P}_t + S_W S_B, \\ \Delta_2 &= S_0S_1\mathcal{P}_t + BS_B + S_w - AS_B, & \Delta_3 &= -\mathcal{A} - S_B, & \Delta_4 &= -1. \end{aligned}$$

The value of  $\mathcal{A} = 2.050$  [5, p. 334],  $B = 0.409$  [26, p. 131] and  $\mathcal{P}_t = 420.19$  measured by NOAA on February 2023.

The dynamic study of (4.16) needs the variable change as  $t = \frac{1}{[H^+]}$ ,  $t \in \mathbb{Z}$ , and  $pH = \log_{10} t$ . Hence, we need to find the solutions of new quartic order polynomial

$$\psi_4(t) = \sum_{k=0}^4 \Delta_{k-4} t^k = 4.3839 \times 10^{-26} t^4 + 4.9091 \times 10^{-17} t^3 + 1.0621 \times 10^{-8} t^2 - 2.05t - 1,$$

which contain the roots

$$\begin{aligned} t_1 &= 1.1970408047866759 \times 10^8, \\ t_2 &= -0.4878048768159488, \\ t_3 &= -6.197530413868866 \times 10^8 + 8.095038662704764i \times 10^7, \\ t_4 &= -6.197530413868866 \times 10^8 - 8.095038662704764i \times 10^7. \end{aligned}$$

Table 7: Results of CFNM for  $\psi_4(t)$  with initial guess  $t_0 = -5 \times 10^8$

$\zeta$	$t^*$	$ t_{n+1} - t_n $	$ \psi(t_{n+1}) $	Iterations
0.90	-6.1975304138e+08+8.0950386627e+07i	9.53674e-07	7.87102e-05	208
0.91	-6.1975304138e+08+8.0950386627e+07i	9.68575e-07	5.94664e-05	163
0.92	-6.1975304138e+08+8.095038662706130e+07i	9.83476e-07	4.13854e-05	128
0.93	-6.197530413e+08+8.095038662e+07i	8.79168e-07	2.93874e-05	101
0.94	-6.197530413e+08+8.0950386627e+07i	8.67856e-07	1.72211e-05	80
0.95	-6.1975304138e+08+8.0950386627e+07i	8.39241e-07	1.13882e-05	64
0.96	-6.1975304138e+08+8.0950386627e+07i	4.80548e-07	6.864633e-06	51
0.97	-6.1975304138e+08+8.0950386627e+07i	6.85453e-07	5.50698e-06	41
0.98	-6.197530413868866e+08-8.0950386627e+07i	6.44722e-07	2.32458e-06	31
0.99	-6.1975304138e+08-8.0950386627e+07i	3.653064e-07	1.45543e-06	23
1	-0.487804876815949	4.16475e-05	0.00	37

In Tables 7 and 8, the solutions of  $\psi_4(t)$  are shown in different order of derivative and faster convergence can be observed in CFDCAWM with minimum error.

Table 8: Results of CFDCAWM for  $\psi_4(t)$  with initial guess  $t_0 = -5 \times 10^8$

$\zeta$	$t^*$	$ t_{n+1} - t_n $	$ \psi(t_{n+1}) $	Iterations
0.90	-6.1975304138e+08+8.0950386627e+07i	9.90675e-07	8.01199e-05	207
0.91	-6.1975304138e+08+8.0950386627e+07i	9.61096e-07	5.84519e-05	163
0.92	-6.1975304138e+08+8.0950386627e+07i	9.83476e-07	4.02239e-05	128
0.93	-6.19753e+08+8.0950386627e+07i	9.68575e-07	2.53841e-05	101
0.94	-6.1975304138e+08+8.0950386627e+07i	9.90675e-07	2.10638e-05	80
0.95	-6.1975304138e+08-8.0950386627e+07i	7.83976e-07	1.18761e-05	64
0.96	-6.1975304138e+08-8.0950386627e+07i	8.34465e-07	6.69969e-06	48
0.97	-6.1975304138e+08-8.0950386627e+07i	1.435547e-06	1.249140e-05	36
0.98	-6.197530413868e+08-8.0950386627e+07i	4.29815e-07	2.53319e-06	28
0.99	-6.1975304138e+08+8.0950386627e+07i	2.53319e-07	2.96409e-06	24
1	-0.487804876815949	0.00231	0.00	07

Table 9: The data  $\mathcal{P}_t$  available from NOAA to calculate the pH of the ocean from 2012-2023 using Whittaker method.

Year	$\mathcal{P}_t$	pH	Year	$\mathcal{P}_t$	pH
2012	394.06	8.1013	2018	408.72	8.0881
2013	396.74	8.0988	2019	411.66	8.0855
2014	398.81	8.0969	2020	414.24	8.0833
2015	401.01	8.0950	2021	416.45	8.0813
2016	404.41	8.0919	2022	418.56	8.0560
2017	406.76	8.0898	2023	420.19	8.0781

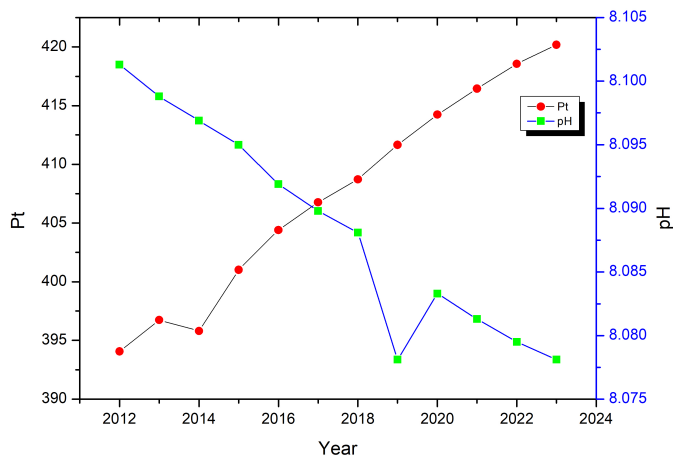


Figure 6: Relation between  $\mathcal{P}_t$  and pH

The pH is calculated in the Table 9 for different values of  $\mathcal{P}_t$  given by NOAA from the year 2012-2023 (February). The graph 6 says about the relation between pH and  $\mathcal{P}_t$ , and it can also be noticed that the pH is inversely proportional to  $\mathcal{P}_t$ .

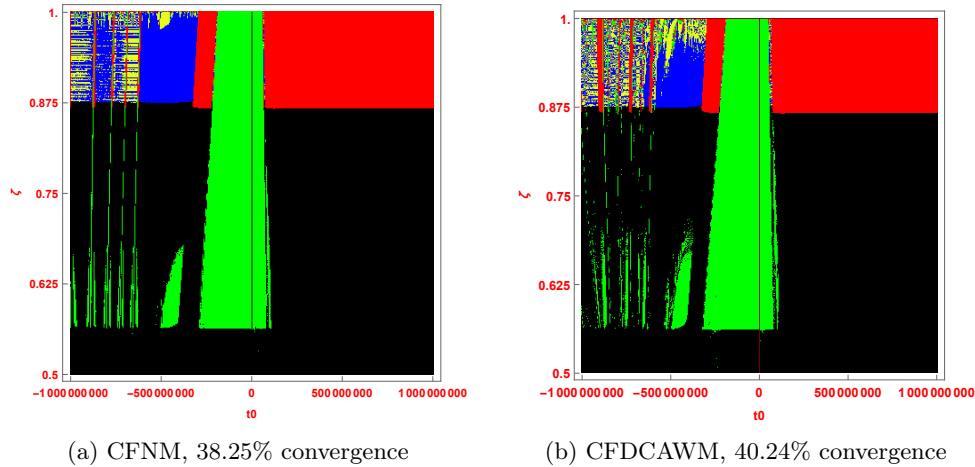


Figure 7: Convergence planes of  $\psi_4(t)$  for real initial guess  $t_0 = a, a \in \mathbb{R}$ .

In Figure 7, the convergence planes of CFNM and CFDCAWM are illustrated. Also, the real root  $t_1 = 1.1970408047866759 \times 10^8$  corresponds to the solution  $[H^+]^* = 8.3539 \times 10^7$  is painted in red color. Moreover, we have found that the  $H^+$  ion concentration in CFDCAWM (40.24%) is more compared to CFNM (38.25%).

**Example 4.5** (Schrödinger wave equation for a hydrogen atom [25]). The location of the electron relative to the core has a probability distribution in quantum mechanics, which is connected to the solution of the Schrödinger wave equation for a charged particle travelling in a Coulomb potential. The classic Schrödinger equation for a single particle of mass  $m$  moving in a central potential is as follows:

$$-\frac{\hbar^2}{2m} \frac{\partial^2 \Psi}{\partial t^2} - K \frac{e^2}{r} \Psi = E\Psi,$$

where  $r$  is the distance of the electron from the core and  $E$  is the energy. And the equation has the following representation in spherical coordinates:

$$-\frac{\hbar^2}{2m} \left[ \frac{1}{r^2} \frac{\partial(r^2 \frac{\partial \Psi}{\partial r})}{\partial r} + \frac{1}{r^2 \sin \theta} \frac{\partial(\sin \theta \frac{\partial \Psi}{\partial \theta})}{\partial \theta} + \frac{1}{r^2 \sin^2 \theta} \frac{\partial^2 \Psi}{\partial \phi^2} \right] + \frac{e^2 \Psi}{r} = E\Psi.$$

The final equation can be divided into an angular equation and a radial equation by applying certain conventional techniques. The angular equation can alternatively be divided into two equations, one of which leads to the corresponding Legendre equation [6]

$$(1 - x^2) \frac{d^2 f}{dx^2} - 2x \frac{df}{dx} + \left( n(n+1) - \frac{m^2}{1-x^2} \right) f(x) = 0.$$

And for  $m = 0$ , i.e. the case of azimuthally symmetric, the equation reduced to Legendre polynomials. So, for our purpose we have taken the obtained form of Legendre equation in the following:

$$\psi_5(t) = 46189t^{10} - 109395t^8 + 90090t^6 - 30030t^4 + 3465t^2 - 63$$

with the roots  $t_1 = -0.9739$ ,  $t_2 = 0.9739$ ,  $t_3 = -0.8651$ ,  $t_4 = 0.8651$ ,  $t_5 = -0.6794$ ,  $t_6 = 0.6794$ ,  $t_7 = -0.4334$ ,  $t_8 = 0.4334$ ,  $t_9 = -0.1489$ , and  $t_{10} = 0.1489$ .

Table 10: Results of CFNM for  $\psi_5(t)$  with initial guess  $t_0 = -1.6$

$\zeta$	$t^*$	$ t_{n+1} - t_n $	$ \psi(t_{n+1}) $	Iterations
0.50	-0.974022883623179	9.934223703655931e-07	0.720438	131
0.55	-0.973979706177354+0.00i	9.767897406476322e-07	0.45272	103
0.60	-0.973952883699453+0.00i	9.894410853972246e-07	0.286638	80
0.65	-0.973934954067361+0.00i	9.675145213883240e-07	0.1757107	63
0.70	-0.973924328185314-0.00i	9.993784602091438e-07	0.1100054	49
0.75	-0.973916963198489-0.00i	9.656237642818866e-07	0.064479	39
0.80	-0.973912597976135+0.00i	9.649762192642797e-07	0.037502	31
0.85	-0.973909751305419-0.00i	9.191366918681609e-07	0.019911	25
0.90	-0.973908232217628+0.00i	9.887810010766884e-07	0.0105259	20
0.95	-0.973906845098482-0.00i	4.377130401467255e-07	0.001955	17
1	-0.973906528517171	8.214154911811988e-10	1.045918e-11	13

Table 11: Results of CFDCAWM for  $\psi_5(t)$  with initial guess  $t_0 = -1.6$

$\zeta$	$t^*$	$ t_{n+1} - t_n $	$ \psi(t_{n+1}) $	Iterations
0.50	-0.974022525194601	9.919475889574870e-07	0.71821	125
0.55	-0.973979997925276+0.00i	9.867753415493397e-07	0.45453	97
0.60	-0.973952593340544-0.00i	9.807070255885009e-07	0.284841	75
0.65	-0.973934897599979+0.00i	9.655019376220153e-07	0.175361	58
0.70	-0.973923495437265-0.00i	9.323057104104748e-07	0.104857	45
0.75	-0.973917138639778+0.00i	9.883953832057202e-07	0.065563	34
0.80	-0.973912010298633+0.00i	8.454325272078123e-07	0.033870	27
0.85	-0.973909290555717+0.00i	7.594809537936342e-07	0.017065	21
0.90	-0.973907816277493+0.00i	7.096176641852026e-07	0.007956	16
0.95	-0.973906956012490-0.00i	6.159379745129812e-07	0.002641	12
1	-0.973906528517169	3.798566096668843e-06	2.346630e-02	07

In Tables 10 and 11, the CFDCAWM provides faster convergence when  $\zeta$  is close to 1. Both the CFNM and CFDCAWM converge to the root  $t_1$  for the initial guess  $t_0 = -1.6$ , but it can be noticed that the CFDCAWM beats the CFNM in the speed of convergence.

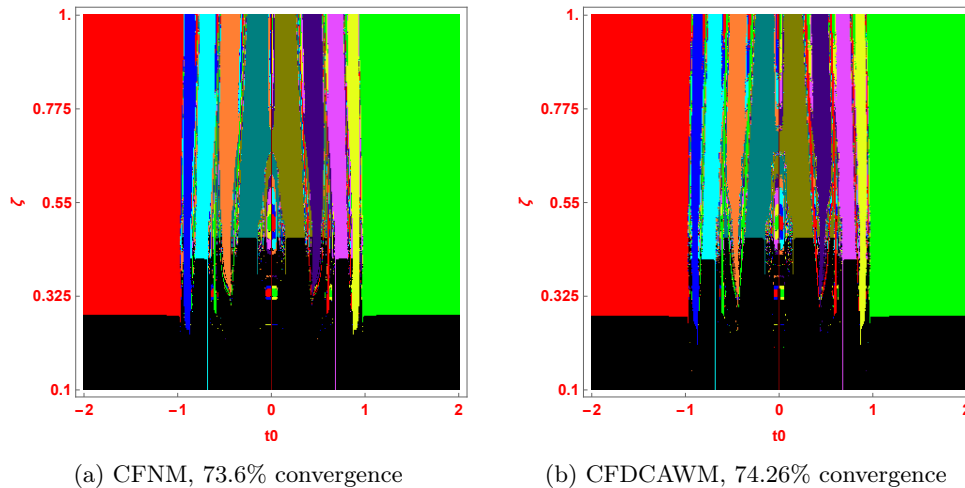


Figure 8: Convergence planes of  $\psi_5(t)$  for real initial guess  $t_0 = a, a \in \mathbb{R}$ .

The convergence plane in Figure 8 gives the CFNM (73.6%) and CFDCAWM (74.26%) percentage of convergence. Moreover, one can find all the roots of  $\psi_5(t)$  by choosing an initial guess in the neighbourhood of zero and changing the order of the derivative in both CFDCAWM and CFNM.

## 5 Conclusion

This research aimed to introduce a new convex acceleration of the fractional Whittaker technique, namely CFDCAWM, in the sense of the Caputo fractional derivative. We have developed the speed of convergence of CFDCAWM to at least  $(1+2\zeta)$ , and we have studied the efficiency and stability of the proposed method. Then, for both CFNM and CFDCAWM, many real-world applications with numerical results are discussed. The convergence planes are illustrated with their convergence percentage for a more straightforward analysis. The results confirmed that CFDCAWM leads CFNM in terms of efficiency and performance.

**Author Contributions:** Both authors have equally contributed to the design and implementation of the research, to the analysis of the results and to the writing of the manuscript.

## References

- [1] P. Agarwal and A. A. El-Sayed, “Vieta-Lucas polynomials for solving a fractional-order mathematical physics model,” *Adv. Difference Equ.*, 2020, Art. ID 626, doi: 10.1186/s13662-020-03085-y.
- [2] A. Akgül, A. Cordero, and J. R. Torregrosa, “A fractional Newton method with  $2\alpha$ th-order of convergence and its stability,” *Appl. Math. Lett.*, vol. 98, pp. 344–351, 2019, doi: 10.1016/j.aml.2019.06.028.
- [3] T. M. Atanacković, S. Pilipović, B. Stanković, and D. Zorica, *Fractional calculus with applications in mechanics*, ser. Mechanical Engineering and Solid Mechanics Series. ISTE, London; John Wiley & Sons, Inc., Hoboken, NJ, 2014.
- [4] D. Babajee and V. Jaunky, “Applications of higher-order optimal Newton secant iterative methods in ocean acidification and investigation of long-run implications of emissions on alkalinity of seawater,” *International Scholarly Research Notices*, vol. 2013, 2013, Art. ID 785287, doi: 10.1155/2013/785287.
- [5] R. Bacastow and C. D. Keeling, “Atmospheric carbon dioxide and radiocarbon in the natural carbon cycle: II. Changes from AD 1700 to 2070 as deduced from a geochemical model,” in *Brookhaven Symposia in Biology*, vol. 24, 1973, pp. 86–135.
- [6] I. N. Bronshtein, K. A. Semendyayev, G. Musiol, and H. Mühlig, *Handbook of mathematics*, 6th ed. Springer, Heidelberg, 2015.
- [7] G. Candelario, A. Cordero, and J. R. Torregrosa, “Multipoint fractional iterative methods with  $(2\alpha + 1)$ th-order of convergence for solving nonlinear problems,” *Mathematics*, vol. 8, no. 3, 2019, Art. ID 452, doi: 10.3390/math8030452.
- [8] M. C. Caputo and D. F. Torres, “Duality for the left and right fractional derivatives,” *Signal Processing*, vol. 107, pp. 265–271, 2015, doi: 10.1016/j.sigpro.2014.09.026.
- [9] S. C. Chapra, *Applied numerical methods with MATLAB for engineers and scientists*, 3rd ed. McGraw-Hill, 2018.
- [10] A. A. El-Sayed and P. Agarwal, “Numerical solution of multiterm variable-order fractional differential equations via shifted Legendre polynomials,” *Math. Methods Appl. Sci.*, vol. 42, no. 11, pp. 3978–3991, 2019, doi: 10.1002/mma.5627.
- [11] J. A. Ezquerro and M. A. Hernández, “Different acceleration procedures of Newton’s method,” *Novi Sad J. Math.*, vol. 27, no. 1, pp. 1–17, 1997.

- [12] W. Gander, "On Halley's iteration method," *Amer. Math. Monthly*, vol. 92, no. 2, pp. 131–134, 1985, doi: 10.2307/2322644.
- [13] K. S. Gritton, J. Seader, and W.-J. Lin, "Global homotopy continuation procedures for seeking all roots of a nonlinear equation," *Computers & Chemical Engineering*, vol. 25, no. 7-8, pp. 1003–1019, 2001.
- [14] G. Honorato and S. Plaza, "Dynamical aspects of some convex acceleration methods as purely iterative algorithm for Newton's maps," *Appl. Math. Comput.*, vol. 251, pp. 507–520, 2015, doi: 10.1016/j.amc.2014.11.083.
- [15] M. K. Jain, S. R. K. Iyengar, and R. K. Jain, *Numerical methods for scientific and engineering computation*, 6th ed. New Age International Publishers, 2012.
- [16] G. Jumarie, "Modified Riemann-Liouville derivative and fractional Taylor series of nondifferentiable functions further results," *Comput. Math. Appl.*, vol. 51, no. 9-10, pp. 1367–1376, 2006, doi: 10.1016/j.camwa.2006.02.001.
- [17] C. Kennedy, "Ocean acidity dissolving tiny snails' protective shell," 2014, [www.climate.gov/news-features/featured-images/ocean-acidity-dissolving-tiny-snails'-protective-shell](http://www.climate.gov/news-features/featured-images/ocean-acidity-dissolving-tiny-snails'-protective-shell) [Accessed: April 5, 2024].
- [18] M. A. Khan, S. Ullah, and M. Farhan, "The dynamics of Zika virus with Caputo fractional derivative," *AIMS Math.*, vol. 4, no. 1, pp. 134–146, 2019, doi: 10.3934/Math.2019.1.134.
- [19] S. Kumar, D. Kumar, J. R. Sharma, C. Cesarano, P. Agarwal, and Y.-M. Chu, "An optimal fourth order derivative-free numerical algorithm for multiple roots," *Symmetry*, vol. 12, no. 6, 2020, Art. ID 1038, doi: 10.3390/sym12061038.
- [20] C. Lanczos, "A precision approximation of the gamma function," *J. Soc. Indust. Appl. Math. Ser. B Numer. Anal.*, vol. 1, pp. 86–96, 1964.
- [21] A. A. Magreñán, "A new tool to study real dynamics: the convergence plane," *Appl. Math. Comput.*, vol. 248, pp. 215–224, 2014, doi: 10.1016/j.amc.2014.09.061.
- [22] V. Morales-Delgado, J. Gómez-Aguilar, K. M. Saad, M. A. Khan, and P. Agarwal, "Analytic solution for oxygen diffusion from capillary to tissues involving external force effects: A fractional calculus approach," *Physica A: Statistical Mechanics and its Applications*, vol. 523, pp. 48–65, 2019, doi: 10.1016/j.physa.2019.02.018.
- [23] Z. M. Odibat and N. T. Shawagfeh, "Generalized Taylor's formula," *Appl. Math. Comput.*, vol. 186, no. 1, pp. 286–293, 2007, doi: 10.1016/j.amc.2006.07.102.
- [24] A. L. Ozores, "Cálculo fraccionario y dinámica newtoniana," *Pensamiento Matemático*, vol. 4, no. 1, pp. 77–105, 2014.

- [25] T. M. Pavkov, V. G. Kabadzhov, I. K. Ivanov, and S. I. Ivanov, “Local convergence analysis of a one parameter family of simultaneous methods with applications to real-world problems,” *Algorithms*, vol. 16, no. 2, p. 103, 2023, Art. ID 103, doi: 10.3390/a16020103.
- [26] J. L. Sarmiento, *Ocean biogeochemical dynamics*. Princeton university press, 2006.
- [27] M. Shams, N. Kausar, C. Samaniego, P. Agarwal, S. F. Ahmed, and S. Momani, “On efficient fractional Caputo-type simultaneous scheme for finding all roots of polynomial equations with biomedical engineering applications,” *Fractals*, vol. 31, no. 04, 2023, Art. ID 2340075, doi: 10.1142/S0218348X23400753.
- [28] P. Tans and R. Keeling, “Trends in atmospheric carbon dioxide, national oceanic & atmospheric administration, earth system research laboratory (noaa/esrl) & scripps institution of oceanography,” 2014, url: <https://gml.noaa.gov/ccgg/trends/data.html>.
- [29] J. Tariboon, S. K. Ntouyas, and P. Agarwal, “New concepts of fractional quantum calculus and applications to impulsive fractional  $q$ -difference equations,” *Adv. Difference Equ.*, 2015, Art. ID 2015:18, doi: 10.1186/s13662-014-0348-8.
- [30] A. Torres-Hernández and F. Brambila-Paz, “Fractional Newton-Raphson method,” *MathSJ*, vol. 8, no. 1, 2021, doi: 10.5121/mathsj.2021.8101.
- [31] J. F. Traub, *Iterative methods for the solution of equations*, ser. Prentice-Hall Series in Automatic Computation. Prentice-Hall, Inc., Englewood Cliffs, NJ, 1964.
- [32] M. A. H. Verón, “An acceleration procedure of the Whittaker method by means of convexity,” *Zb. Rad. Prirod.-Mat. Fak. Ser. Mat.*, vol. 20, no. 1, pp. 27–38, 1990.